

ROWS OF DIMERIC-PARTICLES WITHIN THE AXOLEMMA AND JUXTAPOSED PARTICLES WITHIN GLIA, INCORPORATED INTO A NEW MODEL FOR THE PARANODAL GLIAL-AXONAL JUNCTION AT THE NODE OF RANVIER

CLAYTON A. WILEY and MARK H. ELLISMAN

From the Department of Neurosciences, School of Medicine, University of California at San Diego, La Jolla, California 92093

ABSTRACT

Using freeze-fracture techniques, we have analyzed the glial-axonal junction (GAJ) between Schwann cells and axons in the peripheral nervous system, and between oligodendrocytes and axons in the central nervous system of the rat. We have identified a new set of dimeric-particles arranged in circumferential rows within the protoplasmic fracture faces (P-faces) of the paranodal axolemma in the region of glial-axonal juxtaposition. These particles, 260 Å in length, composed of two 115-Å subunits, are observed in both aldehyde-fixed and nonfixed preparations. The rows of dimeric-particles within the axonal P-face are associated with complementary rows of pits within the external fracture face (E-face) of the paranodal axolemma. These axonal particles are positioned between rows of 160-Å particles that occur in both fracture faces of the glial loops in the same region. We observed, in addition to these previously described 160-Å particles, a new set of 75-Å glial particles within the glial P-faces of the GAJ. These 75-Å particles form rows that are centered between the rows of 160-Å particles and are therefore superimposed over the rows of dimeric-particles within the paranodal axolemma. Our new findings are interpreted with respect to methods of specimen preparation as well as to a potential role for the paranodal organ in saltatory conduction. We conclude that this particle-rich junction between axon and glia could potentially provide an intricate mechanism for ion exchange between these two cell types.

KEY WORDS freeze-fracture · node of Ranvier · intercellular junctions · myelinated axons · Schwann cells · membrane specializations

Over a century ago, Louis-Antoine Ranvier (31, 32, 33) described what has since been known as the node of Ranvier. Despite the limitations of Ranvier's techniques, he developed some hy-

potheses regarding the nature and function of this structure that are still widely accepted today. It continues to be the anatomist's hope that a carefully detailed description of a structure will help define aspects of its function. Since Ranvier's time, the use of new investigative techniques, in particular electron microscopy (EM), has increased our appreciation for the structural complexity of the node of Ranvier. Initially, thin-section EM was

the primary tool for examining the node. Recently, with the refinement of freeze-fracture techniques for showing intercellular junctions and other membrane specializations, the unique morphology of the node of Ranvier has been greatly elaborated (3, 11, 13, 20, 26, 36, 38, 39).

Attempts have been made to integrate the several independent descriptions of the glial-axonal junction (GAJ) (30) although several apparent discrepancies remain. There are at least three likely explanations for these discrepancies: (a) equivalent observations were made but variations in description may have led to different interpretations; (b) variations in freeze-fracture techniques and in the preparation of specimens may have led to different observations; or (c) variations inherent in the structure itself, perhaps depending on its physiologic state at the time of fixation, may have led to different observations. This paper describes morphologic differences associated with alternative methods of freeze-fracture techniques, and incorporates our new observations which together permit an internally consistent description of the glial-axonal junction.

Background

The paranode is defined as the region in which the cytoplasm-containing margins of the myelin lamellae abut the axon. The glial margin wraps around the paranodal axolemma in a helical fashion giving the axon a scalloped border. With freeze-fracture, the region of axolemma at the crest of the scallops (i.e., axolemma apposed to the interstices between the glial loop) consistently displays large particles on both the axonal E-face and axonal P-face (3, 11, 13, 20, 21, 27, 36, 39). In the troughs of the scallops, the glial loops and axolemma are intimately juxtaposed. In conventional thin-section preparations, the slightly undulate glial and axonal membranes in the region of close apposition are separated by ~ 20 – 30 Å (the GAJ cleft), and occasionally are bridged by electron-dense bars, best seen in lead-citrate but not in uranyl-acetate-stained preparations (4, 5, 7, 19, 22).

In freeze-fracture replicas of the region of juxtaposition, Livingston and co-workers (27) found the scalloped axonal E-face to manifest 250- to 300-Å-wide bands after 5 min of etching, while the axonal P-face showed only scattered 50- to 100-Å particles with or without etching. The glial E-face was found to contain 100-Å particles in

rows that were again 250–300 Å apart. The glial P-face showed some 100-Å particles, but only a hint of a linear arrangement. On the basis of their size and regular spacing, Livingston and co-workers hypothesized that the glial E-face particles were profiles of structures that could fit between the axonal E-face bands, possibly involved in a form of ion communication between the two cells. Fig. 1*a* summarizes their findings.

Schnapp and Mugnaini (39) found all four membrane faces in the region of GAJ to contain complementary ridges and grooves. The axonal E-face in Schnapp's replicas was devoid of particles, but on rare occasions a "crystalline array" of paired particles ~ 65 Å in size was observed on the axonal E-face. The subunits constituting the array were small and difficult to resolve, suggesting that they protruded only slightly from the fracture face. The axonal P-face of his preparations contained some 80- to 150-Å particles that occasionally appeared clustered along the ridges of the P-face. The glial faces in this region of glial-axonal juxtaposition were observed to contain 100-Å particles in the grooves of the E-face and in the ridges of the P-face. On the basis of the smooth undulating character of the membrane faces, and a structural analogy with septate junctions, Schnapp and Mugnaini hypothesized, as did Ranvier (31), that the GAJ performed "a mechanical function... suggesting a strong anchorage of the myelin sheath on the axolemma" (reference 39, p. 230). This anchorage would be accomplished by a connection of the particles of the ridges and troughs with "extracellular septa." Though they did "not wish to exclude the possibility that the GAJ might implement some sort of communication between the two cells," analogous to the septate junction, they considered it unlikely that the membrane particles at the GAJ "provide intercellular channels" (reference 40, p. 230). Fig. 1*b* summarizes their findings.

Dermietzel's description (11) of these faces in the cat central nervous system (CNS) shares some features of both of the other investigations. In this work, the axonal E-face in the region of close apposition displayed convex bands 180–240 Å wide which, with low-angle shadowing, were seen to be subdivided into diagonally arranged 40 to 50-Å particles. The complementary axonal P-face was occasionally "represented by parallel running rows of particles which surround particle-free space" (reference, p. 581). In this same region, the

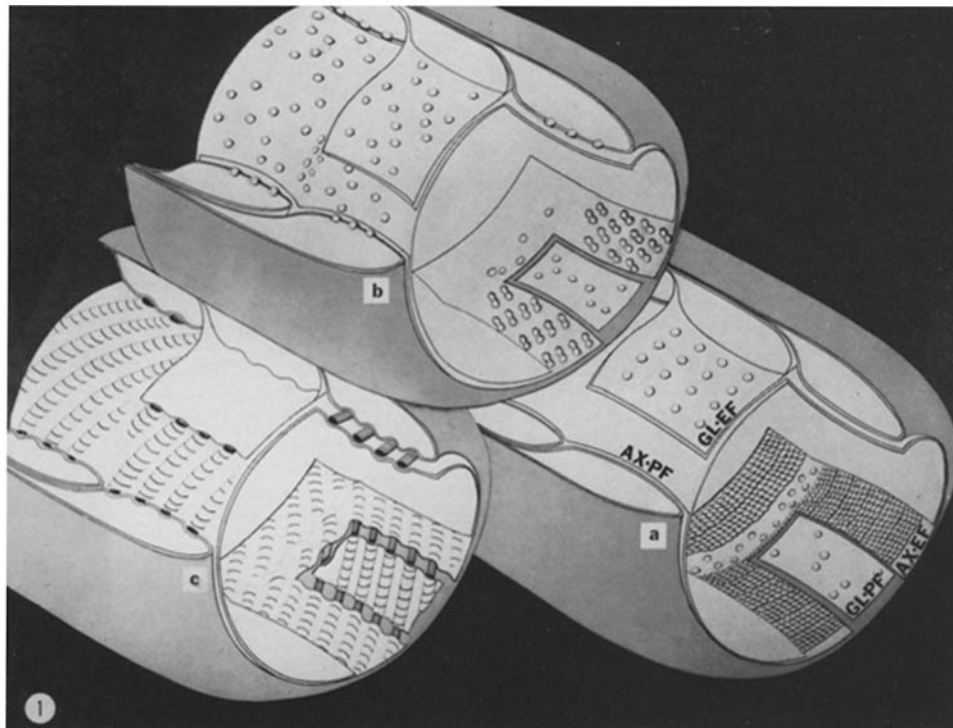


FIGURE 1 (a, b, and c) Summary drawings presenting features of the GAJ as seen in earlier studies. Each three-dimensional projection reveals the same four fracture faces, some differing in interpretation. (a) Livingston and co-workers' (27) scheme of the paranodal region emphasized the junctional membrane specializations of the glial E-face (*GL-EF*) and axonal E-face (*AX-EF*). The glial E-face contained rows of 100-Å particles with a regular inter-row periodicity. The axonal E-face contained bands of 60- to 70-Å diagonal elements. The axonal P-face (*AX-PF*) and glial P-face (*GL-PF*) did not display evidence of an ordered junctional specialization but were reported to contain scattered 50 to 100-Å particles. (b) Schnapp and Mugnaini's (39) scheme of the paranodal region emphasized the nonparticulate character of the axonal E-face of GAJ. In this model, however, the axonal E-face displays the rarely seen crystalline array (40). At the crests of the scallops, both fracture faces of the axolemma exhibited some large particles. Within the scallops, particles 80-150 Å in diameter were observed exclusively in the P-face, while within the glial membrane 160-Å particles were observed in both fracture faces. The glial and axonal membranes were hypothesized to be separated by an extracellular band in which the fracture face particles were embedded. (c) Dermietzel's (11) scheme of the paranodal region emphasized a possible impression made on both membranes by an extracellular transverse band. The transverse bands are 180-240 Å wide and contain diagonal striations (for further details see text).

glial E-face displayed bands broader and flatter than those on the axolemmal E-face, while the glial P-face appeared fairly nondescript. Dermietzel hypothesized that his replicas and thin sections were best interpreted as demonstrating an extracellular transverse band closely shared by the two cells. Like Schnapp and Mugnaini, he suggested that the function of this junction could be adherence and also a possible sealing role limiting the exchange of molecules in the GAJ cleft. Fig. 1c summarizes Dermietzel's findings.

MATERIALS AND METHODS

Standard Aldehyde-fixed Freeze-Fracture Preparations

Sprague-Dawley rats (Hilltop Lab Animals, Inc., Chatsworth, Calif.), from 1 to 30 wk of age, were anesthetized with 10 mg pentobarbital (Nembutal)/100 g body weight. The animals were sacrificed by rapidly replacing their blood by cardiac perfusion with warm oxygenated Krebs-Ringer's solution (with the following composition in mmol/liter: NaCl, 135; KCl, 5.00; MgCl₂, 1.0; CaCl₂, 2.0; Na₂HCO₃, 15.0; Na₂HPO₄, 1.0; glucose, 11.0) to which heparin (0.01%) and xylocaine (0.1%) had been added. (To

control for the possibility that xylocaine caused changes in membrane fracture faces, we have perfused animals without this drug and have observed no changes in the replicas.) After most of the blood had been replaced (as judged by complete liver pallor over ~30 s), the animal was immediately fixed by continued cardiac perfusion with warm 0.15 M cacodylate-buffered, pH 7.2, 2.0% glutaraldehyde, 1% paraformaldehyde. The spinal cord with dorsal and ventral roots attached was quickly dissected free and placed in fresh cold (4°C) fixative for 1 h. After fixation, the dissection was removed from the fixative and placed in cold cacodylate buffer, pH 7.2, for 1 h. The tissue was then glycerinated in a stepwise fashion with cold glycerol solutions (5, 10, 20, and 30% glycerol in 0.15 M cacodylate buffer) to reach a final concentration of 30% glycerol over a period of 1 h where it was then held at 4°C for an additional 2½ h.

Aldehyde-fixed, Suboptimally Frozen

Preparations

To examine the effect of freezing with a nonuniform (suboptimal) rate of ice-crystal nucleation the above procedure was followed except that the tissue was kept in the final 30% concentration at 4°C for only an additional 1 h. The presence of "suboptimal freezing" was operationally defined by observing the presence of large (1,000-Å) ice-crystals.

Non-fixed Glycerol Cryoprotected

Preparations

Animals were anesthetized as described above, then perfused with a 37°C solution of 20% glycerol in 0.15 M cacodylate buffer, pH 7.2. The spinal cord with dorsal and ventral roots attached was quickly dissected free and placed in cold (4°C) cacodylate-buffered 20% glycerol solution for ½ h. The dissection was then placed in 4°C, 30% glycerol solution for an additional 2 h.

Mounting

The dorsal and ventral roots were carefully cut from the spinal cord with an iridectomy scissors. The roots and spinal cord were sized to between 1.5 and 2 mm with a No. 10 scalpel blade. Roots were then stacked one or two high in small piles of a constant size on Balzers gold welled specimen supports (Balzers Corp., Nashua, N. H.) while additional supports were used for spinal cord sections. To prevent dehydration, these were quickly frozen in Freon 22 maintained at its freezing point by liquid nitrogen. To assure a consistent freezing rate, all samples were of equal size, mounted on identical specimen holders, and frozen against the melting phase of the Freon.

Fracturing

Fracturing was performed in a Balzers 300 freeze-etch device equipped with turbo-molecular pump, platinum evaporating electron gun, interlocked quartz crystal thin film monitor (set at 18 Hz), and a time-heat-limited electronic shutter (14). Throughout fracturing, the vacuum was maintained below 2×10^{-6} Torr, while the stage was maintained at -105°C . With random cleavage orientation, the fracture faces of the glial loops juxtaposed to the paranodal axolemma were not frequently exposed. It was found that a greater number of these fracture faces may be exposed if care is taken to orient specimens on the Balzers stage so that cleavage propagates at right angles to the longitudinal axis of the axon.

After a platinum layer ~20 Å thick was deposited at an angle of 45° , a carbon layer 400–1,000 Å thick was evaporated vertically to provide stability. The replicas were then floated on 20% glycerol in distilled water, and cleaned for 24 h in bleach (Purex), 12 h with 20% chromic acid, followed by careful rinsing in distilled water.

Etching

Etched specimens were fractured at -100°C . The knife was positioned above the specimens for 1–5 min after the last cleavage. Methods of replication and cleaning for etched specimens were the same as described above.

Viewing

Replicas were examined at 80 KV with a JEOL 100CX electron microscope equipped with a eucentric goniometer stage (JEOL USA, Electron Optics Div., Medford, Mass.). Only mature nodes with at least ten layers of compacted myelin (43) were photographed for this study.

RESULTS

We have categorized our observations according to whether or not the specimens were fixed, etched, or optimally cryoprotected. Each category will be subdivided into separate descriptions of the four fracture faces belonging to the glial and axonal membranes that contribute to the GAJ. With replicas that show fracture faces of both glia and axon together, we will illustrate the relative position of the junctional features. At the end of this section, a summary diagram is included to facilitate comparison of the axonal and glial faces as they appear after the different preparative procedures.

Freeze-fracture Morphology of the Paranodal GAJ after Paraformaldehyde-Glutaraldehyde Fixation and Glycerol Cryoprotection,

Without Etching

MORPHOLOGY OF THE AXONAL P-FACE WITHIN THE PARANODAL ZONE (WITH FIXATION AND WITHOUT ETCHING)

The P-face of the paranodal axolemma displays a shallow scalloped border beneath the overlying glial loops (Fig. 2). The width of the scallop varies with the length of the apposed glial loop. These scallops appear to be profiles of a wide (0.1–0.4 μm) helical indentation in the axolemma. The depth of the scallops varies over the length of the paranode, and in large nodes where many glial loops are retracted the scalloping may be discontinuous. Though some large, 100- to 350-Å particles can be found randomly distributed within the P-face of the paranodal axolemma, the greatest

concentration of large particles is found between scallops where the axolemma is apposed to the interstices between the glial loops (arrows, Fig. 2).

REGION OF GLIAL-AXONAL JUXTAPosition: *Particle Rows.* Within the scallops of the axonal P-face are rows of dimeric-, 260-Å-long particles in all nonetched replicas (Fig. 3a). These rows of particles are identifiable in the first five scallops nearest the nodal membrane of all nodes but appear less consistently in the remaining scallops. The rows adopt a narrow angle (10°-20°) relative to the scallop. The rows do not cross from one scallop to the next but rather terminate at the edge of the scallop in which they have begun (circle, Fig. 3a). In regions where the scalloping is absent, the particles are also absent. These particles are most regularly seen associated with scalloped regions close to the nodal membrane and less frequently seen within scallops towards the interparanodal boundary (Fig. 2).

Dimeric-Particles. The dimeric-particles within each row of the axonal P-face are spaced 200 Å apart. At higher magnifications, the particles forming the rows appear as a dimer composed of two similar elliptical subunits each 115 Å in length and 75 Å in width (Fig. 3b). Within each row the dimeric-particles appear diagonally oriented at an angle of ~45° with respect to the row. Where several rows appear within one scallop, the diagonally oriented particles in one row are colinear with dimeric-particles in an adjacent row along the 45° angle. The density of dimeric-particles in these regions of close packing is ~1,500/μm² (i.e., 3,000 of the 115- × 75-Å subunits/μm²).

This description is also consistent with our observation of the axonal P-face of the central nervous system nodes as seen in our spinal cord preparations (Fig. 3c). It should be noted that these particles are quite distinct from the random large particles described in previous studies (11, 27, 39). Though they are of approximately the same dimension and configuration as those infrequently described by Schnapp and Mugnaini (39), they are on a different fracture face.

MORPHOLOGY OF THE AXONAL E-FACE WITHIN THE PARANODAL REGION (WITH FIXATION AND WITHOUT ETCHING)

The E-face of the paranodal axolemma appears scalloped in a manner complementary to the axonal P-face. Large, 100- to 300-Å particles of the axolemmal E-face are generally concentrated in regions apposed to the interstices between glial

loops, as in the P-face (Fig. 4, large arrows). When the angle of platinum shadowing is close to the axon's longitudinal axis, circumferential ridges 350 Å in width are often visible. In regions of excellent cryoprotection, these ridges appear as faint undulations due to platinum deposition along the sides of the ridge (Fig. 5). These regions can be appreciated as rows of pits distributed the same as the dimeric-particles in the axonal P-face (Figs. 4 and 5). This undulating pattern in the axonal E-face is more pronounced in regions of suboptimal freezing (Fig. 6). This may be a product of membrane collapse due to dehydration resulting from ice crystal formation (37).

MORPHOLOGY OF THE E-FACE OF THE JUXTANEURONAL GLIAL LOOP (WITH FIXATION AND WITHOUT ETCHING)

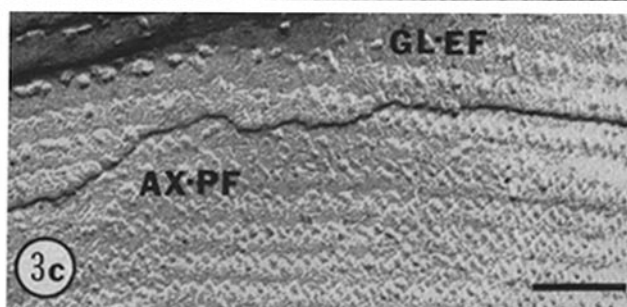
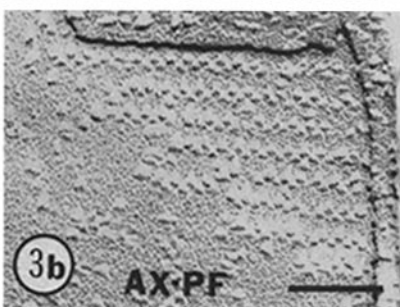
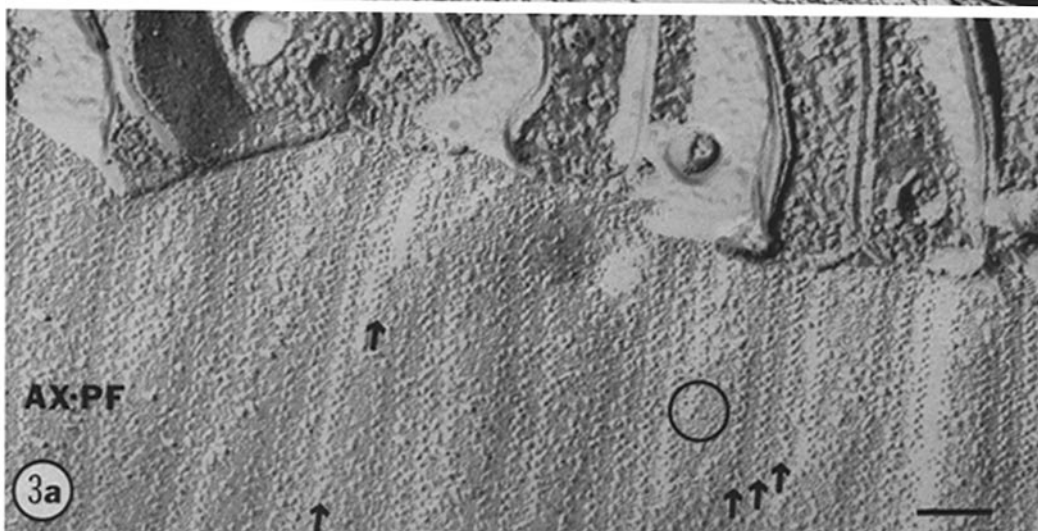
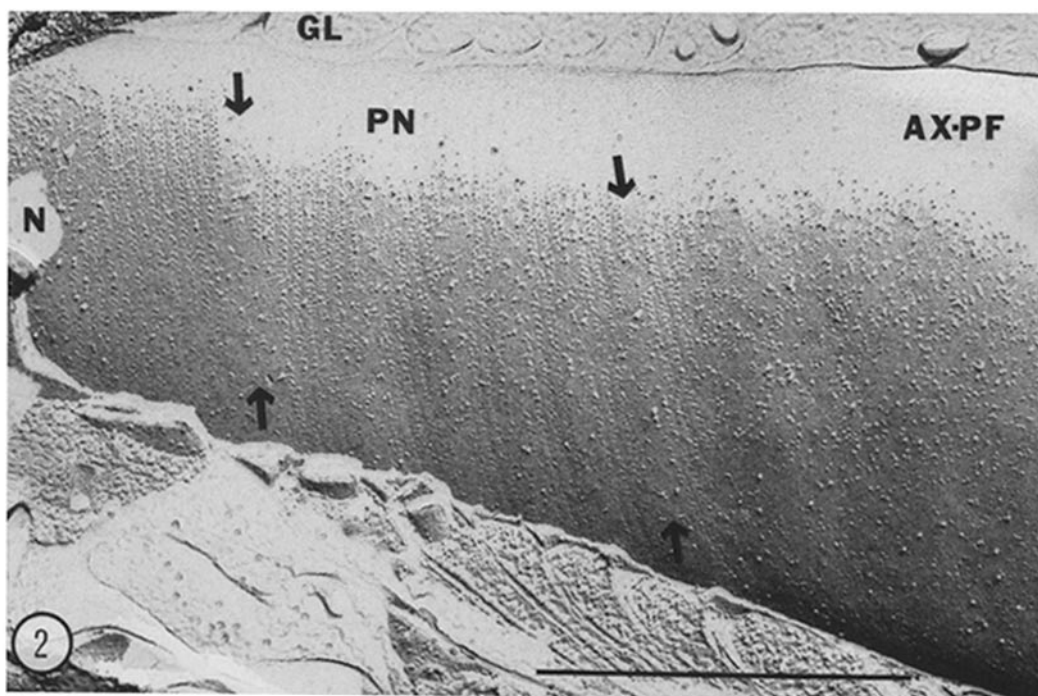
The E-face of the glial loop contains rows of large, 160-Å particles coursing at a 10°-20° angle to the axis of the winding glial loops (Fig. 7). The particle rows are 360 Å apart. The particles in each row have an equal tendency to fracture with the E-face as with the P-face, but where several particles are present in the glial E-face they are separated by 200 Å (center-to-center). Tilting the replica in the eucentric goniometric stage shows that these large particles are tall enough to extend across the 20- to 30-Å space of the glial-axonal junction.

MORPHOLOGY OF THE P-FACE OF THE JUXTANEURONAL GLIAL LOOPS (WITH FIXATION AND WITHOUT ETCHING)

The glial loop P-face contains an equal fraction of the same large (160-Å) particles as described for glial E-face (Fig. 8). A row of 75-Å particles is centered between the rows of larger particles in the P-face. The 75-Å particles are spaced ~100 Å apart. In some replicas, the rows composed of these smaller particles adopt a ropelike appearance (Fig. 10).

RELATIVE POSITION OF FEATURES ON GAJ FACES (WITH FIXATION AND WITHOUT ETCHING)

In fortunate replicas where the fracture plane has jumped between glial and axonal faces, it is possible to compare positions of features on the axonal face with positions of features on the glial face. Because of distortions inherent in the projection of a nonhorizontal surface (i.e., the paranode) onto a horizontal photographic plate, the evalua-



tion of the relative position of these elements necessitates stereoscopy, or evaluation of images determined to be flat projections.

AXONAL P-FACE AND GLIAL E-FACE: The dimeric-particle rows of the axonal P-face are found to be positioned between the rows of 160-Å particles in the glial E-face (Fig. 9). The particles composing the rows within the two faces are identically spaced (200 Å). A precise analysis of the relative positions was performed by extrapolating the relative position of particles in one set of rows with respect to particles in the other set of rows by using transparent overlays. This analysis showed that the 160-Å particles are positioned between the rows of dimeric-particles. Here they reside adjacent to the ends of dimeric-particles and are co-linear with the diagonally oriented particles of adjacent rows. This positioning is illustrated in Figs. 9 and 19.

AXONAL E-FACE AND GLIAL P-FACE: The pits corresponding to the dimeric-particles of the axonal P-face are preserved in only the most lightly shadowed areas. Where such areas were found with an adjacent glial P-face exhibiting the rows of 160-Å particles and rows of 75-Å particles, an analysis similar to that described for the two complementary faces (see above) can be performed (Fig. 10; see diagram Fig. 19). This analysis showed that the rows of pits left on the axonal E-face by the dimeric-particles are immediately juxtaposed to the rows of 75-Å particles of the glial P-face and are centered between the larger rows of 160-Å particles. Occasionally, in this position, juxtaposed to the rows of 160-Å glial particles, there is a ridge in the axonal E-face, positioned between the rows of pits (see Fig. 19). The presence of these axonal E-face ridges is enhanced by short periods of etching (see below).

Freeze-fracture Morphology of the Paranodal GAJ after Fixation and Glycerol

Cryoprotection, with Etching

We etched to determine the relationship between the new features of the glial-axonal junction reported above and those reported earlier in studies where etching was employed to enhance certain features (3). These etched preparations provide another image of the GAJ from which the alignment of elements between glia and axon fracture faces may be determined.

MORPHOLOGY OF THE AXONAL P-FACE WITHIN THE PARANODAL ZONE (AFTER FIXATION AND ETCHING)

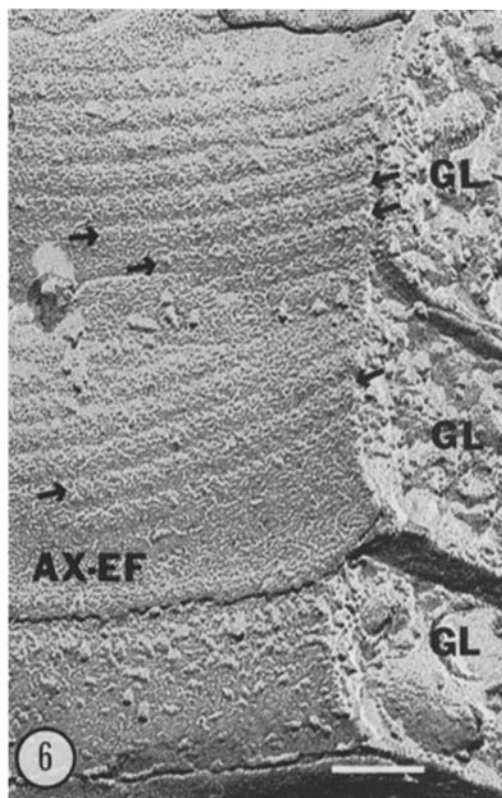
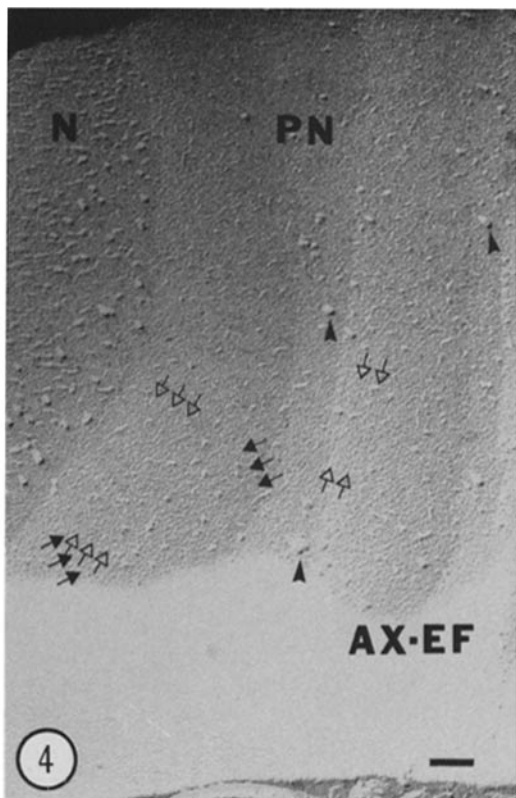
Whereas the scalloped appearance of the axonal P-face remains with etching (up to 5 min), the dimeric-particle rows within the scallops are increasingly obscured with increasing length of etching. After 2 min of etching, the dimeric attribute of the particles is difficult to assess in regions where it was always evident in nonetched preparations (Fig. 11). With more prolonged etching (5 min), the particle rows begin to adopt the appearance of ridges with troughs intervening, making the fracture face within the scallop appear slightly undulated. In those preparations etched for 5 min, <20% of the scallops neighboring the nodal axolemma displayed clear dimeric-particle rows.

MORPHOLOGY OF AXONAL E-FACE WITHIN THE PARANODAL ZONE (AFTER FIXATION AND ETCHING)

The scallops in the axonal E-face are seen with and without etching. Large particles remain visible predominantly between scallops in regions where the axolemma is apposed to the interstices between glial loops (Fig. 12).

FIGURE 2 An axonal P-face (*AX-PF*) after fixation but without etching. The paranodal region (*PN*) of the axon is scalloped beneath the overlying glial loops (*GL*). Large, 100- to 300-Å particles appear in greatest concentration between the scallops (arrows) and in the nodal region (*N*). 12-d-old rat. Bar, 1 μ m. \times 50,000.

FIGURE 3 (*a*, *b*, and *c*) Axonal P-faces after fixation but without etching. (*a*) Rows of particles (arrows) are seen coursing at a narrow angle across the scallop. The termination of a row at the edge of a scallop is encircled. 150-d-old rat. Bar, 1,000 Å. \times 100,000. (*b*) At higher magnifications, the particles are seen to be composed of two similar elliptical subunits diagonally oriented at an angle of 45° with respect to the row. Regions between scallops contain large irregular particles. 150-d-old rat. Bar, 1,000 Å. \times 125,000. (*c*) High-power micrograph of equivalent particles in the axonal P-face (*AX-PF*) of the rat central nervous system demonstrating the generality of this specialization. The overlying glial E-face (*GL-EF*) is also shown. 150-d-old rat. Bar, 1,000 Å. \times 125,000.



After 2 min of etching, indented bands, ~250 Å in width, are found within the scallops (corresponding to the rows of pits left by the dimeric-particles of the axonal P-face). These indented bands are separated from each other by a ridge ~100 Å wide (Fig. 13). After 5 min of etching, these ridges appear to correspond to the broader, ropelike diagonal features of Livingston and co-workers' (27) preparations (Fig. 14).

MORPHOLOGY OF THE E-FACE OF THE Juxtaneuronal Glial Loops (After Fixation and Etching)

After etching for 2 min, the rows of 160-Å particles in the glial E-face appear less distinct (Fig. 11). With 5 min of etching, the particle rows appear as undulations with occasional particulate interruptions.

MORPHOLOGY OF THE P-FACE OF THE Juxtaneuronal Glial Loops (With Fixation and Etching)

As with the glial E-face, etching results in an undulated appearance of glial P-face, occasionally interrupted by large 160-Å particles (Fig. 15). The rows of smaller 75-Å particles visible in the nonetched glial P-face (above) were not visible after etching.

RELATIVE POSITION OF FEATURES ON GAJ FACES AFTER ETCHING (WITH FIXATION AND ETCHING)

AXONAL P-FACE AND GLIAL E-FACE: The

rows of the axonal P-face are found to be positioned between the 160-Å glial particle rows as in the nonetched material.

AXONAL E-FACE AND GLIAL P-FACE: Because a distinctive and defined fine structure is seen in the axonal E-face of etched specimens, it is of value to compare the relationship between etched features and glial P-face features in replicas where both are exposed. We find the ropelike ridges of the axonal E-face to be centered in direct apposition to the 160-Å particle rows on the glial P-face (Figs. 10, 11, and 15, as well as Figs. 18 and 19).

Freeze-fracture Morphology of the Paranodal GAJ after Glycerol Cryoprotection without Fixation and without Etching

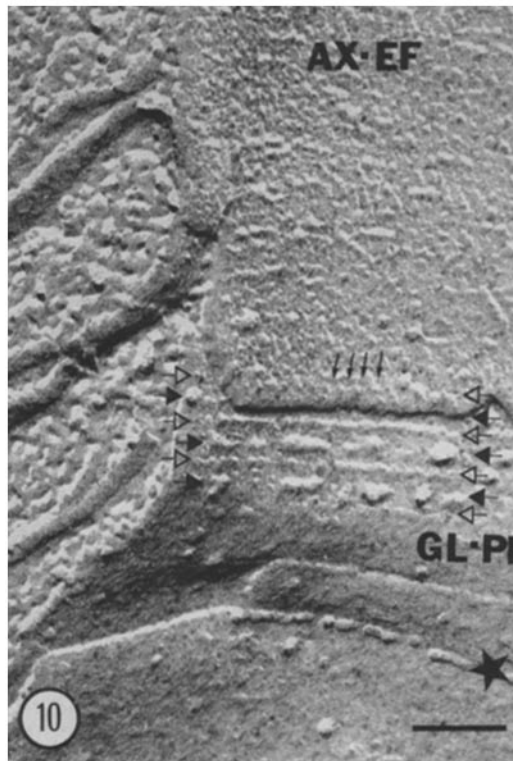
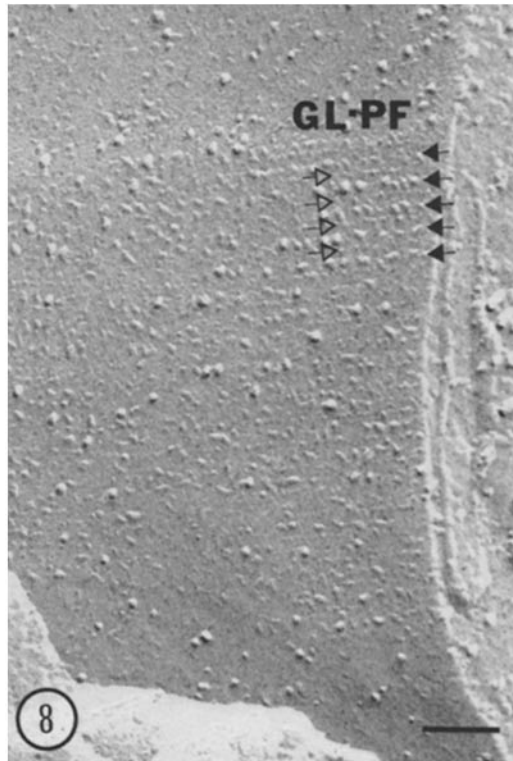
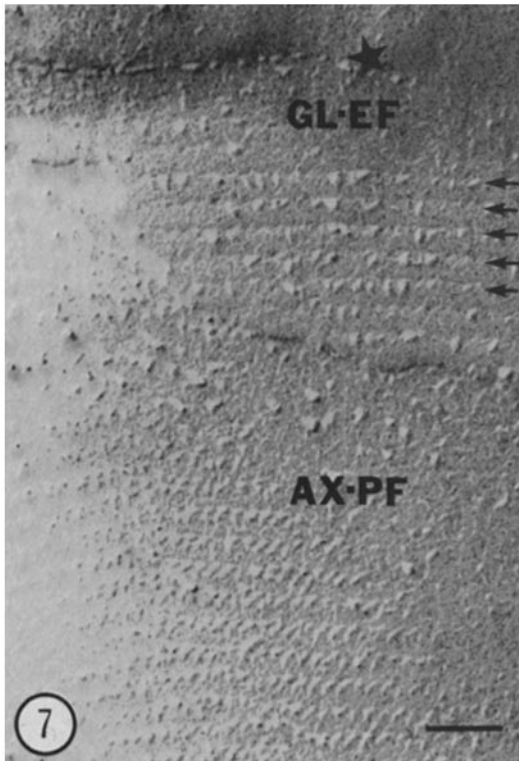
MORPHOLOGY OF THE AXONAL P-FACE WITHIN THE PARANODAL ZONE (WITHOUT FIXATION AND WITHOUT ETCHING)

The axonal P-face displays scallops in which the rows of dimeric-particles are less linear, and more irregular than those seen in fixed material (Fig. 16). Occasionally, rows within one scallop are not parallel to one another. In some areas, dimeric-particles and large (200-Å) particles appear dispersed across the axonal P-face. This more random distribution of particles often results in the interruption of the dimeric-particle rows.

FIGURE 4 An axonal E-face (*AX-EF*) after fixation but without etching. The paranodal region (PN) of the axon is scalloped beneath the overlying glial loops. Large, 100- to 300-Å particles (filled arrowheads) appear most concentrated between scallops. Rows of pits are distributed as were rows of dimeric-particles in axonal P-face. These pits are seen to be oriented along two axes. The one marked by open arrows represents the circumferential axis of impressions of the rows of dimeric-particles while the one marked by closed arrows represents the second axis of co-linearity between the diagonally disposed particles of adjacent rows. 14-d-old rat. Bar, 1,000 Å. $\times 55,000$.

FIGURE 5 A stereopair of micrographs of a paranodal region of the axonal E-face (*AX-EF*) after fixation but without etching. The two images can be fused with the unaided eye (with a little practice) or with a stereo viewer. (Two-lens stereo viewers of satisfactory quality [$\times 2$] are available from Abrams Instrument Corp., Lansing, Mich.) When this is done, a three-dimensional view of the replicated fracture face can be seen and the rows of pits corresponding to rows of dimeric-particles (large arrows) are more readily visualized. Small arrows point to individual pits. 150-d-old rat. 5° tilt; $\times 82,500$ or 145,000 with a $\times 2$ stereo viewer.

FIGURE 6 An axonal E-face (*AX-EF*) frozen at a suboptimal freezing rate after fixation but without etching. The undulated and crosshatched pattern in the axonal E-face may be due to membrane collapse onto an extracellular structure. Glial loops (*GL*) contain large ice-crystals. 150-d-old rat. Bar, 1,000 Å. $\times 125,000$.



MORPHOLOGY OF THE AXONAL E-FACE
WITHIN THE PARANODAL ZONE (WITHOUT
FIXATION AND WITHOUT ETCHING)

Without fixation, the paranodal axonal E-face is scalloped as it was with fixation. A few large (200- to 300-Å) particles appear more concentrated at the tops of the scallops. As with the fixed material, this fracture face displays circumferential ridges 350 Å wide when the direction of shadowing is nearly parallel to the axon's longitudinal axis.

MORPHOLOGY OF THE E-FACE OF THE
JUXTANEURONAL GLIAL LOOP (WITHOUT
FIXATION AND WITHOUT ETCHING)

The nonfixed glial E-face displays rows of large (160-Å) particles as it did in fixed material.

MORPHOLOGY OF THE P-FACE OF THE
JUXTANEURONAL GLIAL LOOP (WITHOUT
FIXATION AND WITHOUT ETCHING)

The nonfixed glial P-face displays an equal portion of the 160-Å particles forming rows that are shared with the glial E-face. The rows of smaller (75-Å) particles are also still seen between the rows of 160-Å particles in the glial P-face as in the fixed (but not in the etched) preparations.

*Freeze-fracture Morphology of the Paranodal
GAJ after Glycerol Cryoprotection and
Etching, without Fixation*

With increasing times of etching, the nonfixed material changes in a manner similar to that noted after the etching of fixed material. In summary, after etching there is a decrease in the distinctiveness of particles on the axonal P-face and both glial faces, while there is an increase in the distinctiveness of a banded pattern in the axonal E-face (Fig. 17). This banding of the axonal E-face appears to correspond to the circumferential ridges seen in the nonetched preparations.

A diagrammatic representation of the four fracture faces after the different preparative procedures is presented in Fig. 18.

*Freeze-fracture Morphology of the Node of
Ranvier in the Above Preparations*

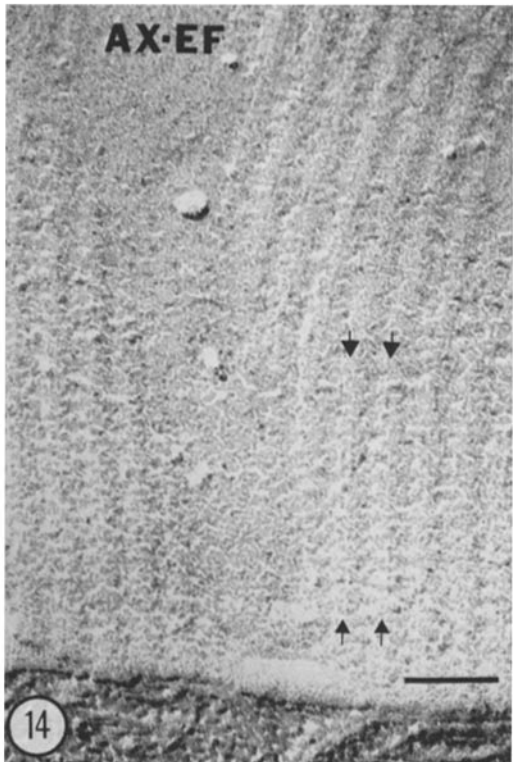
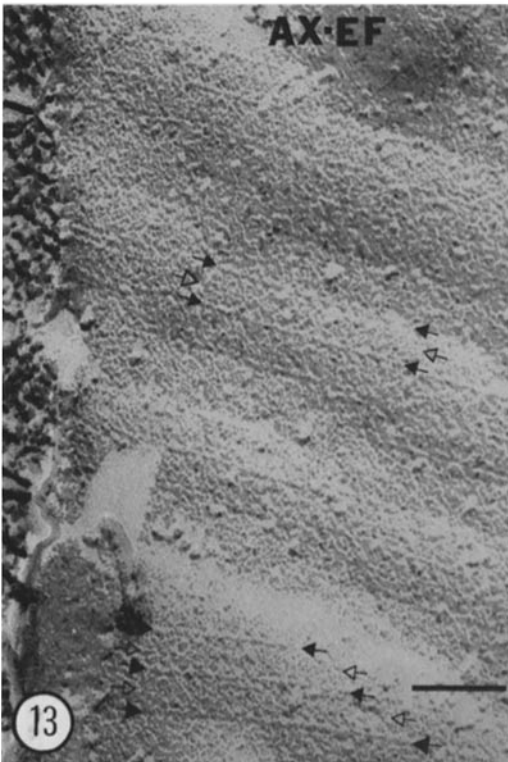
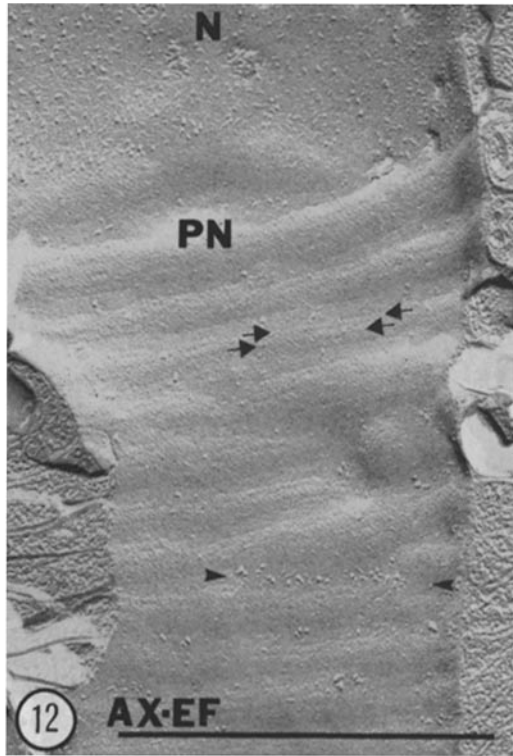
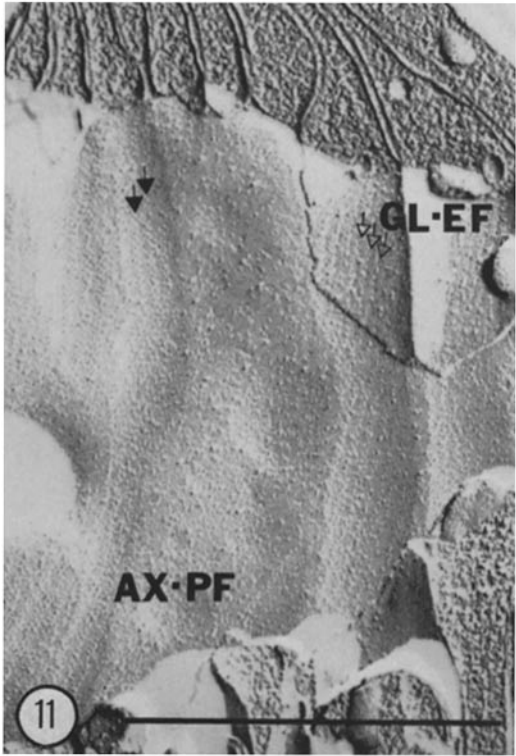
In contrast to the paranodal faces, the appearance of the nodal E-face and P-face in all of the above preparations is qualitatively quite similar. The nodal faces of all fixed preparations are found to contain heterogeneously-sized particles of sizes and densities per square micron similar to those described by previous workers (12, 13, 21). In unfixed preparations, the E-face appears to con-

FIGURE 7 An E-face of a glial loop (*GL-EF*) displaying rows of 160-Å particles. The rows (arrows) are spaced 360 Å apart while the particles within the rows are separated by 200 Å. The underlying axonal P-face (*AX-PF*) exhibits the rows of dimeric particles. A star indicates the location of a tight junction between adjacent glial loops. 10-d-old rat. Bar, 1,000 Å. $\times 100,000$.

FIGURE 8 A P-face of a terminal glial loop (*GL-PF*) displaying rows of 160-Å particles (filled arrows). The rows are spaced 360 Å apart, while the particles within the rows are separated by 200 Å. Rows of 75-Å particles (open arrows) are centered between the rows of 160-Å particles. 10-d-old rat. Bar, 1,000 Å. $\times 100,000$.

FIGURE 9 In a series of transparent overlays, micrographs such as that shown here have been used to project the position of axonal specializations with respect to glial specializations. The rows (arrows) of dimeric-particles in the axonal P-face (*AX-PF*) are seen to be positioned between the rows of 160-Å particles in the glial E-face (*GL-EF*) (arrowheads). The 160-Å glial particles fall on a line of colinearity between dimeric-particles of adjacent rows (see text and Fig. 19). 12-d-old rat. Bar, 1,000 Å. $\times 125,000$.

FIGURE 10 Using transparent overlays as in Fig. 9, it is possible to project the position of specializations on the axonal E-face (*AX-EF*) with respect to specializations on the glial P-face (*GL-PF*) in this fixed and nonetched preparation. Rows of large glial particles (closed arrows) alternate with rows of small glial particles (open arrows). The rows of small glial particles are superimposed over the obscure pits of the axonal E-face (indicated by small arrows), while the row of large glial particles are superimposed over the ridges of the axonal E-face. A star indicates the position of a tight junction between adjacent glial loops. 14-d-old rat. Bar, 1,000 Å. $\times 125,000$.



tain a greater proportion of the elongate (100-Å × 250-Å) particles than the fixed nodal E-face.

Summary of Results

(a) The scalloped axonal P-face in our fixed and nonfixed preparations displays circumferential rows of diagonally oriented dimeric-particles. Where several rows appear within one scallop, the diagonally oriented dimeric-particles in one row are colinear with the diagonal orientation of the dimeric-particles in an adjacent row. (This line of colinearity between dimeric-particles is at an angle of 45° to the row.)

(b) The dimeric-particle rows of the axonal P-face are positioned between the rows formed by the 160-Å particles in the glial E-face. The center-to-center spacing between particles in both glial and axonal rows is equivalent (200 Å).

(c) The 160-Å glial particles are intercalated between adjacent rows of axonal dimeric-particles and lie on the line of colinearity between the rows of diagonally oriented axonal particles.

(d) The nonetched glial P-face displays rows of small (75-Å) particles between the previously reported rows of 160-Å particles in both fixed and unfixed preparations.

(e) With increased etching, the particle rows on the axonal P-face and both glial faces become obscure, lending an undulated appearance to the fracture faces.

(f) The axonal E-face in the paranodal region shows a system of ridges and troughs without etching only if the platinum shadowing is at a low angle and is perpendicular to the ridges.

(g) The axonal E-face ridges are juxtaposed to the glial P-face rows of large (160-Å) particles.

(h) After etching, the axonal E-face demonstrates bands composed of pitted oval subunits. The orientation, size, and location of these pitted bands indicate that they are complementary to the newly described dimeric-particles, of the axonal P-face.

(i) These observations are consistent for both central nervous system and peripheral nervous system tissue.

DISCUSSION

Attempts to integrate the observations from earlier studies of paranodal structure have met with difficulties (cf. reference 30). Our observations demonstrate that variations in specimen preparation techniques (i.e., fixation, cryoprotection, angle of fracture plane relative to angle of axon's longitudinal axis, etching, and tilt angle of replica relative to photographic plate) can account for differences among earlier observations.

Fixation

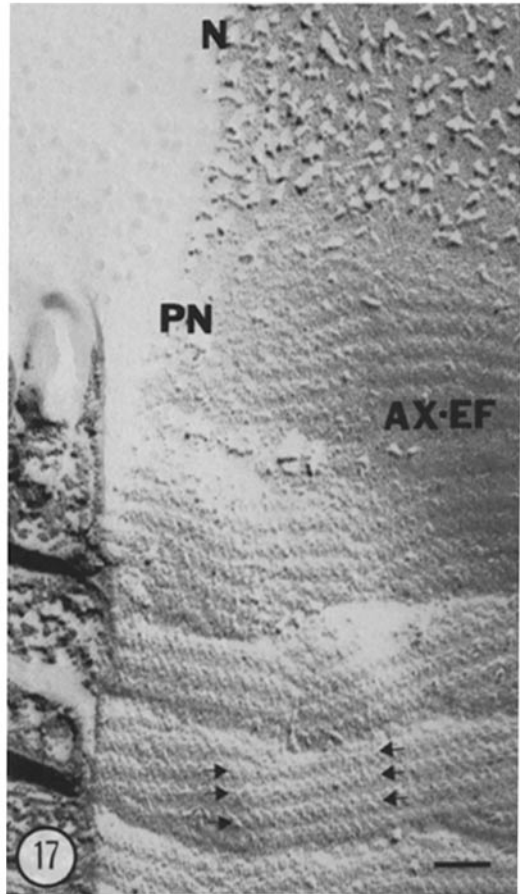
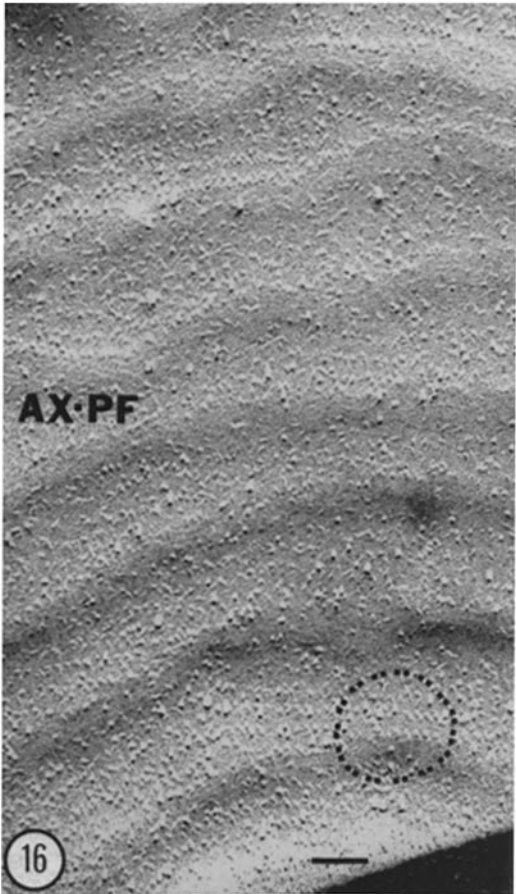
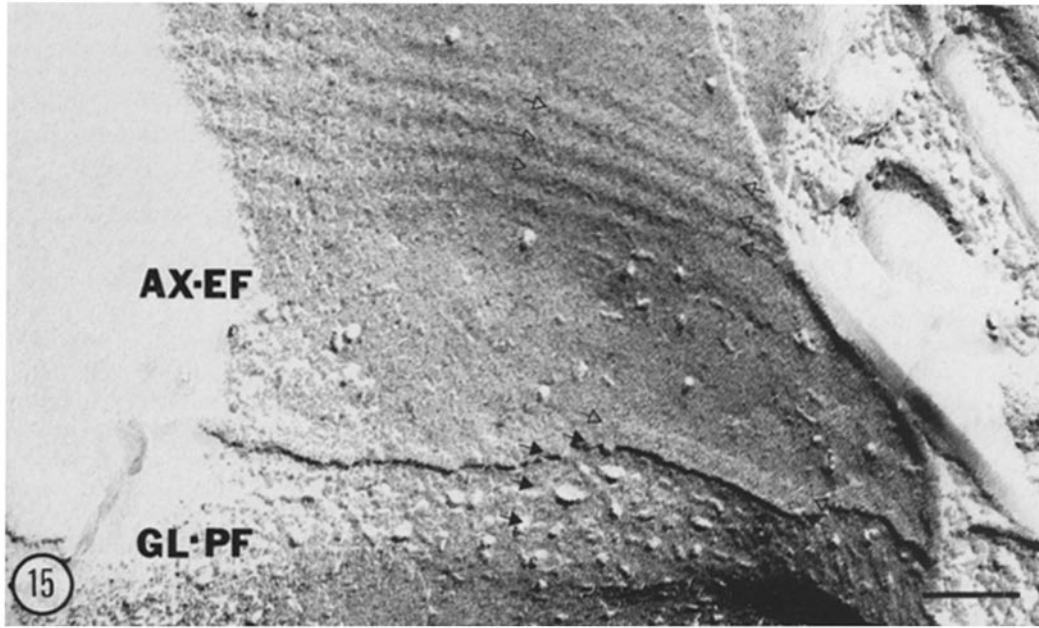
The node of Ranvier has been found by some investigators to be a labile structure (6). Changes in the presence and partitioning in fracture faces depending on variations in fixation have been reported in other systems (10). Though our dimeric-particles on the axonal P-face are present with and without fixation and though there is no clear change in particle partitioning, the stability of the circumferential rows is definitely enhanced by aldehyde-fixation. It is possible that the fixation procedures used by other investigators resulted in movement of particles either into less observable positions, into less identifiable configurations, or even into another fracture face (10, 39). In addi-

FIGURE 11 An axonal P-face (*AX-PF*) after fixation and 2 min of etching. Within the scallops, this face appears slightly undulated. The rows of dimeric-particles on the axonal P-face (filled arrows) and the rows of 160-Å particles in the glial E-face (*GL-EF*) (open arrows) appear less distinct than they did in nonetched preparations. 14-d-old rat. Bar, 1 μm. × 50,000.

FIGURE 12 An axonal E-face (*AX-EF*) after fixation and 2 min of etching. Large particles (arrowheads) are occasionally present between the scallops of the paranodal membrane (*PN*). Rows of pits (arrows) complementary to the dimeric-particles of the axonal P-face are still visible in this micrograph. A portion of the nodal E-face (*N*) is also seen to the left of the paranode. 14-d-old rat. Bar, 1 μm. × 50,000.

FIGURE 13 An axonal E-face (*AX-EF*) after fixation and 2 min of etching. Narrow ridges (filled arrows) are seen between 250-Å indented bands (open arrows). 14-d-old rat. Bar, 1,000 Å. × 125,000.

FIGURE 14 An axonal E-face (*AX-EF*) after fixation and 5 min of etching. The narrow ridges of the 2-min etch preparations appear to have been transformed into broader rope-like ridges (filled arrows). 10-d-old rat. Bar, 1,000 Å. × 125,000.



tion, there may be species-related differences in the partitioning of the dimeric particles seen here in P-faces of rat peripheral and central nerves and a possibly related "crystalline array" associated with the axonal E-faces of turtle CNS tissue as noted by Schnapp and co-workers (40).

Cryoprotection

Freezing of tissue can result in ice-crystal damage when the rate of freezing is less than that necessary for rapid homogeneous nucleation of ice crystals. The rate necessary for such freezing can be lowered to readily obtainable values by diminishing the sample size and by cryoprotection of the tissue. Cryoprotection of peripheral nerve tissue with a 30% glycerol soak for 2 h appears to result in excellent preservation and minimal tissue damage when conventional freezing techniques are employed. Extracellular ice-crystal formation is one example of a frequently encountered problem when the rate of freezing is below that necessary for optimal vitrification. With the formation of extracellular ice-crystals, tissue dehydration, and membrane collapse can occur. Collapse of glial and axonal membranes can result in the observations of undulated fracture faces. When we intentionally froze specimens in a less than optimal manner (see Materials and Methods), paranodal membranes showed undulated faces and obscured membrane particles. A balance has to be achieved, however, since fracturing characteristics may be affected by very long glycerol incubations.

Angle of Fracturing

We do not see any qualitative differences in the membrane faces of specimens fractured at different angles. However, the presence of different faces, depending upon angle of cleavage relative

to the nerve axis, suggests that propagation of the fracture plane can vary with different forms of cleavage.

Etching

A possible "decoration" effect and membrane collapse are two changes in membrane morphology hypothesized to occur with etching. Using ultrahigh vacuum (10^{-9} Torr) freeze-fracture, Gross and co-workers (17) introduced pure water vapor after freeze-fracturing specimens and demonstrated decoration of specific regions of membranes. With the loss of water from tissue samples that have been fractured, membranes have been shown to collapse onto extracellular structures (37). The similarities between our etched and suboptimally frozen specimens (see above) suggest that the changes in the morphology of axonal E-faces that occur with etching are probably due to membrane collapse onto an extracellular structure. The presence of extracellular densities in the GAJ along with our observations of the size and position of the glial 160-Å particle rows suggest that it is collapse onto these structures that convolutes the axonal E-faces.

Differences in Tilt Angle of Replicas Relative to the Photographic Plate

When one is analyzing the relative position of particles on different membrane faces, micrographs can be misinterpreted if not viewed stereographically. The goniometric stage provides for the taking of stereo electron micrographs and these allow precise relative positioning of features on the glial and axonal fracture faces. Therefore, we consider our matching of features between glia and axon fracture faces to supersede earlier observations.

FIGURE 15 An axonal E-face (*AX-EF*) and glial P-face (*GL-PF*) after fixation and 5 min of etching. Matching the rope-like ridges of the etched axonal E-face (open arrows) with the rows of 160-Å particles of the glial P-face (closed arrows) demonstrates that the ridges are superimposed over the rows of 160-Å particles (see Figs. 18 and 19). 8-d-old rat. Bar, 1,000 Å. $\times 125,000$.

FIGURE 16 An axonal P-face (*AX-PF*) without fixation and without etching. Within the scallops, the rows of dimeric-particles are less linear and more irregular than those seen in fixed material (cf. Fig. 3a). In some areas (circled), dimeric-particles and large (200-Å) particles appear to interrupt the dimeric-particle rows. 14-d-old rat. Bar, 1,000 Å $\times 75,000$.

FIGURE 17 An axonal E-face (*AX-EF*) without fixation and after 5 min of etching. The rope-like bands (arrows) within the scalloped paranodal region (*PN*) are clearly demarcated from the nodal region (*N*) of the axolemma. 14-d-old rat. Bar, 1,000 Å. $\times 75,000$.

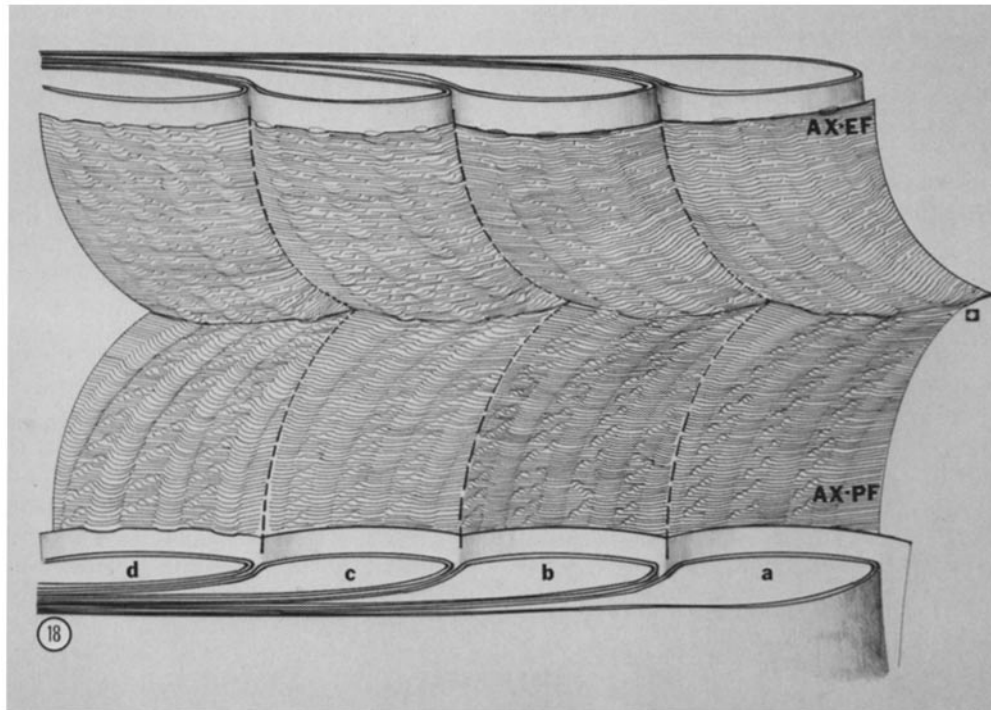


FIGURE 18 Schematic diagrams of both axonal fracture faces in the GAJ are shown peeled apart after the following preparative procedures: (a) After fixation, but without etching. The axonal P-face (AX-PF) displays rows of dimeric-particles spaced 200 Å apart. A slight depression coursing along the side of the rows can be appreciated when shadowing is at a low angle. Within each row the dimeric-particles are diagonally oriented at an angle of $\sim 45^\circ$ with respect to the row and are colinear along the 45° angle with dimeric-particles in adjacent rows. The dimeric-particles are composed of two similar elliptical subunits, each 115 Å in length and 75 Å in width. The axonal E-face in these preparations displays rows of pits when the platinum-shadowing angle is optimal. The position, orientation, and size of these pits are compatible with their being complementary to the dimeric-particles of the axonal P-face. A slight expression coursing along the sides of the rows can be appreciated when shadowing is at a low angle. (b) Without fixation and without etching. The fracture faces of the axon are similar to those of fixed preparations, except for small areas in which the linearity of the dimeric-particle rows is disrupted. (c) After fixation and 5 min of etching. The dimeric-particle rows are obscured in the axonal P-face. The axonal E-face is undulated with rope-like ridges, ~ 250 Å in width, that are separated by shallow dimeric-pits. These particulate ridges are presumably an impression of the extracellular structures (glial particles) resulting from the dehydration of the extracellular space that occurs during etching. (d) After fixation and without etching but suboptimally frozen. Both fracture faces of the axolemma appear undulated, possibly a product of dehydration of the small extracellular spaces in the GAJ that occurs during freezing. The banding of the axonal E-face is similar to that in the etched preparations, while the axonal P-face shows a banding that is not as apparent in etched preparations.

Synthesis of the Four Membrane Faces into a Model of the Paranodal Structure

The complementary appearance of glial E-faces and P-faces allows for their matching. This facilitates reconstruction of the relationship among all four faces involved in the GAJ. Because the glial E-faces and P-faces display rows of 160-Å particles

spaced at multiples of 200 Å, we concur with other workers that, in the intact glial membrane, particles occur in a single row with a regular spacing of 200 Å. Upon cleavage, there is an approximately equal tendency for the particles to fracture with either the E-face or P-face (partition coefficient of unity). This suggests that the macromolecule represented by the intramembrane particle has a

roughly equal association with both sides of the glial membrane (24). The dimeric-particle rows within the P-face of the axolemma, as well as rows of pits within the E-face of the axolemma, lie between the 160-Å particle rows of the glial faces. The rows of 75-Å particles in glial P-faces are superimposed above the rows of dimeric-particles in the axonal P-face.

Experiments with lanthanum staining of the GAJ demonstrate nonlanthanum-permeated spaces, 140- to 190-Å wide, separated by a distance similar to the spacing of glial particle rows (11, 19). These non-lanthanum-permeated spaces appear to stain with lead in other thin-section preparations (5, 23). These findings coupled with later observations of large 160-Å glial particles suggest that a macromolecular bridge crosses the narrow gap (20–30 Å) between glia and axon. In support of this connection, the 160-Å glial particles appear to span the extracellular space when viewed stereographically at high tilt. Fig. 19 is a model for the GAJ that represents a synthesis of these data. This model highlights the adjacent relationship between the dimeric-particles of the axolemma and the 160-Å glial particles, as well as the direct superposition of the smaller rows of 80-Å glial particles over these same dimeric-particles.

Implications of Structure on Function at the Node of Ranvier

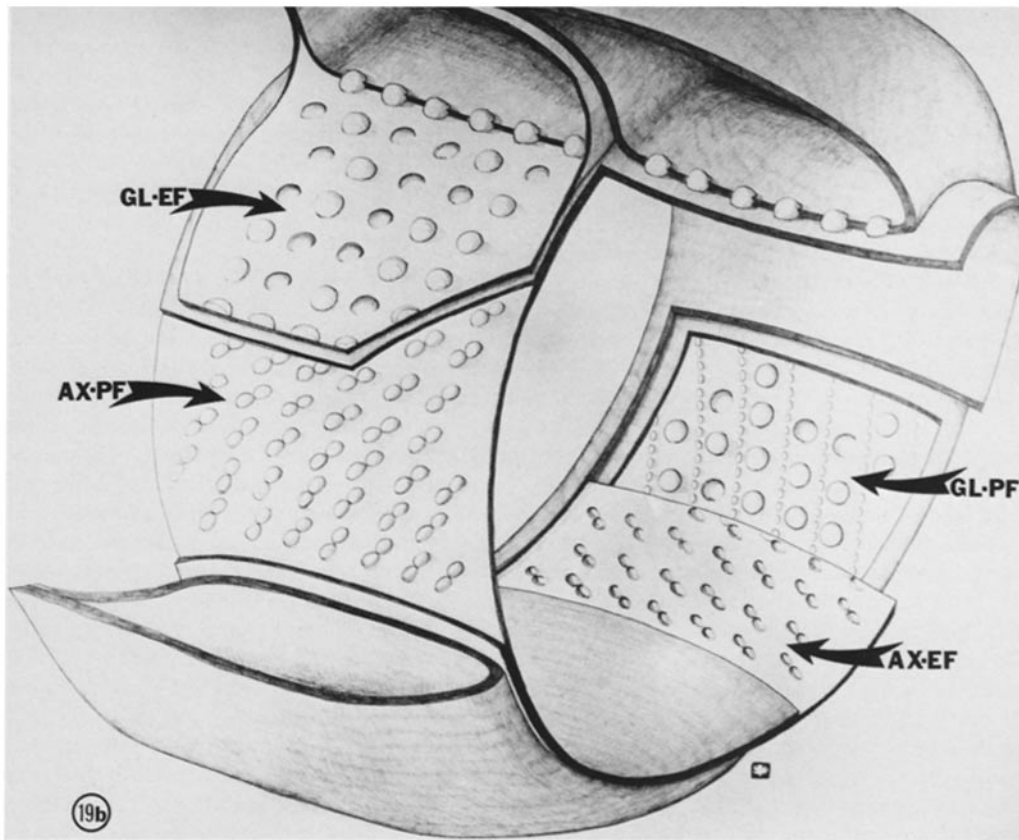
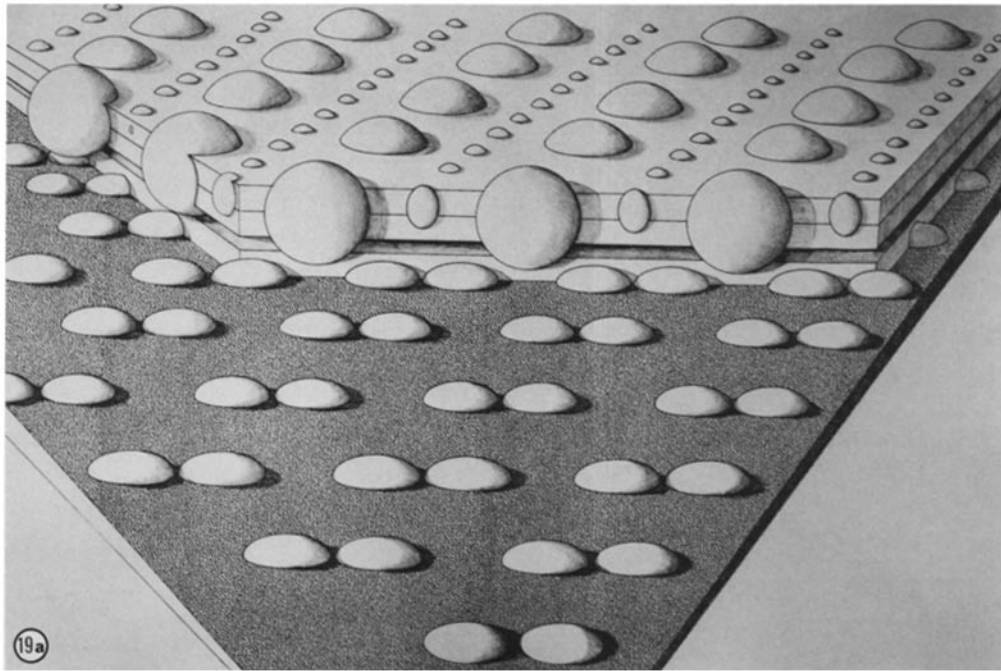
A model for saltatory conduction was first proposed by Lillie in 1925 (26). The model developed into a hypothesis for impulse conduction in myelinated nerve reviewed early by Frankenhaeuser (16). Most of the transmembrane ion movement in this model is thought to occur at the node, with myelin acting passively to increase transmembrane resistance and decrease membrane capacitance throughout the internodal region. Though this theory received considerable support from physiologic studies, modern recordings with bipolar-electrodes allow the determination of the position of transmembrane current only to within ~0.1 mm (34). Thus, the electrophysiological activity is localized to a range that is several orders of magnitude larger than the size of the node. Despite limitations in the precision of electrophysiologic measurements, a theory of saltatory conduction with the bare nodal membrane as the site of inward current gained general acceptance. As discussed above, early thin-section and freeze-fracture studies were interpreted to support the role of the node

in transmembrane ion movement, and the role of the glial cell as contributing to the insulation of the internodal region. More recent analyses of the structure of the node of Ranvier have complicated this interpretation (1, 18). Staempfli's (41) morphometric measurement of nodal membrane capacitance was found to differ by 10- to 30-fold from that calculated on the basis of electrophysiologic measurements. These investigators concluded that more area than the bare node must be involved in saltatory conduction.

Using electrophysiologic estimates of the conductance of single sodium channels in frog myelinated nerves, Nonner and co-workers (29) estimated that if all Na⁺ current were restricted to the nodal region there would be ~5,000 channels/μm² of frog nodal membrane. After elimination of slow inactivation of sodium conductance with *Leiurus* scorpion venom, noise spectra analysis (8) demonstrates 10⁵ sodium channels/node. Pharmacological measurements of radioactive saxitoxin bindings suggest the concentration of sodium channels in the rabbit nodal membrane to be ~8,000–10,000/μm² (35). These pharmacological measurements also assumed that the binding component was contained only in the bare nodal region. On the basis of estimates of a size of 250,000 daltons for a single tetrodotoxin (TTX) binding component (Na channel?) from *Electrophorus electricus* (2, 25), its solubility and other physical properties, one would expect the Na channel to be exposed by freeze-fracture as a particle ~70–100 Å in diameter.

With the above correlations, we could expect to find the nodal membrane to contain 5,000–12,000, ~70- to 100-Å particles/μm², if the sodium channels were confined to this region. However, quantitative analysis of bare nodal membrane fracture faces (12, 13, 21) yields a total of little more than 2,000 heterogeneously-sized particles. The number of these heterogeneous particles that could participate as sodium channels is further diminished by recent immunohistochemical studies (44) showing localization of Na/K ATPase (a 90- to 100-Å freeze-fracture particle [9]) to nodal membrane. Thus, if the sodium channel is confined to the nodal region at the estimated density of 5,000–12,000, it either is not exposed by fracturing or exists in a multimeric form.

In summary, these studies suggest that the bare nodal membrane is too small to exclusively contain the sodium channel. The ability of the myelinated frog nerve to produce an action potential when the



nodal membrane is bathed in a low sodium (0.05 mM) solution (42) implies that the sodium necessary for the inward current must come from a source other than the extracellular fluid around the node. These observations coupled with the high concentration of sodium in the paranodal glial loops (15) have led us to propose that this is the source of sodium for the early current of an action potential. The importance of the paranodal organ in the production of an action potential is further strengthened by evidence indicating a differential sensitivity of the nodal complex to precisely positioned laser damage (28, 42). Small lesions in the paranodal region result in loss of early sodium current during excitation (28). These studies suggest a possible alteration in our conception of the role of different membrane regions in saltatory conduction.

Certainly the function of the paranodal region as a simple source of nerve insulation is not implied in its structure. Why should such a large portion of the axonal surface ($\frac{1}{20}$ to $\frac{1}{10}$ of the internodal area) be involved in a leaky (as shown by tracer studies) junction when a series of tight junctions would accomplish a task of insulation more readily? The elaborate axonal E-face observed by Livingston and co-workers (27) suggested a more specialized function for the paranodal axolemma. The size of our dimeric-particles is compatible with the hypothesis that they are sodium channels. Though it is not reasonable to directly compare the density from earlier studies since the earlier estimates are predicated on the confinement of the sodium channel to the nodal membrane, it is pertinent to compare absolute number of channels predicted by the earlier density estimates for a comparably sized node. These

comparisons show a good match of total number of subunits of dimeric-particles and predicted number of sodium channels in exemplary nodes. We hypothesize that the proximity of the dimeric-particles to the glial membrane specializations implies a functional interaction between the glia and axon. This evidence along with our recent studies on the localization of sodium to the glial loops suggests an intimate communication with possible direct or indirect sodium exchange between these cells.

We are very grateful to Dana R. Livingston for patience and expertise in the creation of the illustrations. We thank Dr. L. Andrew Staehelin for his support and thoughtful critique of this work.

Much of this work was made possible by generous contributions from Hoffman La-Roche Inc., to Robert B. Livingston, enabling the purchase of the electron microscope. This work was supported by a grant to M. H. Ellisman from the Muscular Dystrophy Association of America and National Institutes of Health Grant NS14718. C. A. Wiley was supported by National Institute of General Medical Sciences training grant PHS GM07198.

Received for publication 30 April 1979, and in revised form 6 August 1979.

REFERENCES

1. ABBOTT, B. C., A. V. HILL, and J. V. HOWARTH. 1958. The positive and negative heat production associated with a nerve impulse. *Proc. R. Soc. B. Biol. Sci.* **148**:149-187.
2. AGNEW, W. S., S. R. LEVINSON, J. S. BRABSON, and M. A. RAFTERY. 1978. Purification of the tetrodotoxin-binding component associated with the voltage sensitive sodium channel from *Electrophorus electricus* electroplax membranes. *Proc. Natl. Acad. Sci. U. S. A.* **75**:2606-2610.
3. AKERT, K., C. SANDRI, R. B. LIVINGSTON, and H. MOOR. 1974. Extracellular spaces and junctional complexes at the node of Ranvier. In *Actualites Neurophysiologiques*. A. M. Monnier, editor. Masson et Cie, Paris. 9-22.

FIGURE 19 (a) This schematic diagram illustrates the relative positions of GAJ features in the glial and axonal membranes as described in Results. The glial membrane contains alternating rows of large (160-Å) particles and rows of small (75-Å) particles. The rows of small particles are superimposed over the rows of dimeric-particles of the axolemma. The rows of large glial particles are therefore superimposed over the interval between adjacent rows of axonal dimeric-particles. Overlays on the freeze-fracture micrographs have demonstrated that the 160-Å glial particles are intercalated between the rows of diagonally oriented axonal particles. (b) This diagram is a three-dimensional model of the GAJ, synthesizing our freeze-fracture observations. The relative positions of particles on the axonal P-face (AX-PF), axonal E-face (AX-EF), glial E-face (GL-EF), and glial P-face (GL-PF) are shown. The axonal P-face contains circumferential rows of dimeric-particles that do not cross from one scallop to the next, but rather terminate at the edge of the scallop in which they have begun. Complementary rows of pits are shown in the axonal E-face. The glial P-face and E-face displays rows of 160-Å particles and pits. The glial P-face shows additional rows of 75-Å particles positioned between the rows of larger particles, and superimposed over the rows of dimeric-pits in the axonal E-face.

4. ANDRES, K. H. 1965. Über die Feinstruktur besonderer Einrichtungen in markhaltigen Nervenfasern des Kleinhirns der Ratte. *Z. Zellforsch. Mikrosk. Anat.* **65**:701-712.
5. BARGMANN, W. and E. LINDNER. 1964. Ueber den Feinbau des Nebennierenmarkes des Igels (*Erinaceus europaeus* L.). *Z. Zellforsch. Mikrosk. Anat.* **64**:868-912.
6. BLANK, W. F., JR., M. B. BUNGE, and R. P. BUNGE. 1974. The sensitivity of the myelin sheath, particularly the Schwann cell-axolemmal junction, to lowered calcium levels in cultured sensory ganglia. *Brain Res.* **67**: 503-513.
7. BUNGE, M. B., R. P. BUNGE, E. R. PETERSON, and M. R. MURRAY. 1967. A light and electron microscope study of long-term organized cultures of rat dorsal root ganglia. *J. Cell Biol.* **32**:439-466.
8. CONTI, B. F., B. HILLE, B. NEUMCKE, W. NONNER, and R. STAMPFLI. 1976. Conductance of the sodium channel in myelinated nerve fibers with modified sodium inactivation. *J. Physiol.* **262**:729-742.
9. DEGUCHI, N., P. L. JORGENSEN, and A. B. MAUNSBACH. 1977. Ultrastructure of the sodium pump. *J. Cell Biol.* **75**:619-634.
10. DEMPSEY, G. P., S. BULLIVANT, and W. B. WATKINS. 1973. Endothelial cell membranes: polarity of particles as seen by freeze-fracturing. *Science (Wash. D. C.)* **179**:190-192.
11. DERMETZEL, R. 1974. Junctions in the central nervous system of the cat. II. A contribution to the tertiary structure of the axonal-glia junction in the paranodal region of the node of Ranvier. *Cell Tissue Res.* **148**:577-586.
12. ELLISMAN, M. H. 1976. The distribution of membrane molecular specializations characteristic of the node of Ranvier is not dependent upon myelination. In Sixth Annual Meeting of the Society for Neurosciences, Bethesda, Md. 2:410.
13. ELLISMAN, M. H. 1979. Molecular specializations of the axon membrane at nodes of Ranvier are not dependent upon myelination. *J. Neurocytol.* **8**. In press.
14. ELLISMAN, M. H., and L. A. STAEHELIN. 1979. An electronically interlocked electron gun shutter for preparing improved replicas of freeze-fracture specimens. In *Freeze Fracture: Methods, Artifacts, and Interpretations*. J. E. Rash and C. S. Hudson, editors. Raven Press, Inc., N. Y.
15. ELLISMAN, M. H., P. FRIEDMAN, and W. HAMILTON. 1979. Cytochemical localization of cations in myelinated nerve using TEM, HVEM, SEM, and electron probe microanalysis. In *Scanning Electron Microscopy 1979: An International Review of Advances in Biological Techniques and Applications of the Scanning Electron Microscope*. R. P. Becker and O. Johari, editors. AMF O'Hare, Ill. 793-800.
16. FRANKENHEUSER, B. 1952. The hypothesis of saltatory conduction. *Cold Spring Harbor Symp. Quant. Biol.* **17**:27-32.
17. GROSS, H., D. KEUBLER, E. BOS, and H. MOOR. 1978. Decoration of specific sites on freeze-fractured membranes. *J. Cell Biol.* **79**:646-656.
18. HILL, A. V., and F. V. HOWARTH. 1958. The initial heat production of stimulated nerve. *Proc. R. Soc. B. Biol. Sci.* **149**:167-175.
19. HIRANO, A., and H. M. DEMBITZER. 1969. The transverse bands as a means of access to the periaxonal space of the central myelinated nerve fiber. *J. Ultrastruct. Res.* **28**:141-419.
20. KRISTOL, C., K. AKERT, C. SANDRI, U. R. WYSS, M. V. L. BENNETT, and H. MOOR. 1977. The Ranvier nodes in the neurogenic electric organ of the knife fish *Sternarchus*: a freeze-etching study on the distribution of membrane-associated particles. *Brain Res.* **125**:197-212.
21. KRISTOL, C., C. SANDRI, and K. AKERT. 1978. Intramembranous particles at the nodes of Ranvier of the cat spinal cord: a morphometric study. *Brain Res.* **142**:391-400.
22. LAATSCH, R. H., and W. M. COWAN. 1966. A structural specialization at nodes of Ranvier in the central nervous system. *Nature (Lond.)* **210**: 757-758.
23. LASANSKY, A. 1969. Basal junctions at synaptic endings of turtle visual cells. *J. Cell Biol.* **40**:577-581.
24. LEFORT-TRAN, M., T. GULIK, H. PLATTNER, J. BEISSON, and W. WEISSNER. 1978. Influences of cryofixation procedures on organization and partition of intramembrane particles. Ninth International Congress on Electron Microscopy, Toronto. 2:146-417.
25. LEVINSON, S. R., and J. C. ELLORY. 1973. Molecular size of the tetrodotoxin binding site estimated by irradiation inactivation. *Nat. New Biol.* **245**:122-123.
26. LILLIE, R. S. 1925. Factors affecting transmission and recovery in the passive iron nerve model. *J. Gen. Physiol.* **7**:473-507.
27. LIVINGSTON, R. B., K. PFENNINGER, H. MOOR, and K. AKERT. 1973. Specialized paranodal and interparanodal glial-axonal junctions in the peripheral and central nervous system: a freeze-etching study. *Brain Res.* **58**:1-24.
28. MÜLLER-MOHNSSEN, H., A. TIPPE, F. HILLENKAMP, and E. UNSOLD. 1974. Is the rise of the action potential at the Ranvier node controlled by a paranodal organ? *Naturwissenschaften*. **61**:369-370.
29. NONNER, W., E. ROJAS, and R. STAMPFLI. 1975. Gating currents in the node of Ranvier: voltage and time dependence. *Philos. Trans. R. Soc. Lond. B. Biol. Sci.* **270**:483-492.
30. PETERS, A., S. L. PALAY, and H. DEF. WEBSTER. 1976. *The Fine Structure of the Nervous System*. W. B. Saunders Co., Philadelphia, Penn. 406.
31. RANVIER, L. 1874. De quelque faits relatifs à l'histologie et à la physiologie des muscles striés. *Arch. Physiol. Norm. Pathol.* 2 Ser. 1:5-15.
32. RANVIER, M. L. (1878) *Leçons Sur L'Histologie du Systeme Nerveux*. Paris, F. Savy.
33. RANVIER, L. (1880) *Leçons d'Anatomie Generale sur le Systeme Musculaire*. Delahaye, Paris.
34. RASMINSKY, M., and T. A. SEARS. 1972. Internodal conduction in undissected demyelinated nerve fibers. *J. Physiol. (Lond.)* **227**:323-350.
35. RITCHIE, J. M., and R. B. ROGART. 1977. Density of sodium channels in mammalian myelinated nerve fibers and nature of the axonal membrane under the myelin sheath. *Proc. Natl. Acad. Sci. U. S. A.* **74**: 211-215.
36. ROSENBLUTH, J. 1976. Intramembranous particle distribution at the node of Ranvier and adjacent axolemma in myelinated axons of the frog, brain. *J. Neurocytol.* **5**:731-745.
37. SANDRI, C., J. M. VAN BUREN, and K. AKERT. 1977. Membrane morphology of the vertebrate nervous system. A study with freeze-etch technique. *Prog. Brain Res.* **46**:384.
38. SCHNAPP, B., C. PERACCHIA, and E. MUGNAINI. 1973. Freeze-fracture of Ranvier nodes. *J. Cell Biol.* **59**(2, Pt. 2):360a. (Abstr.).
39. SCHNAPP, B., and E. MUGNAINI. 1975. The myelin sheath. Electron microscopic studies with thin section and freeze-fracture. In *Golgi Centennial Symposium Proceedings*. Raven Press, Inc., N. Y. 209-230.
40. SCHNAPP, B., C. PERACCHIA, and E. MUGNAINI. 1976. The paranodal axo-glia junction in the central nervous system studied with thin sections and freeze-fracture. *Neuroscience*. **1**:181-190.
41. STAMPFLI, R. 1954. Saltatory conduction in nerve. *Physiol. Rev.* **34**: 101-112.
42. TIPPE, A., and H. MÜLLER-MOHNSSEN. 1975. Further experimental evidence for the synapse hypothesis of Na⁺ current activation and inactivation at the Ranvier node. *Naturwissenschaften*. **62**:490-491.
43. WILEY, C. A., and M. H. ELLISMAN. 1979. Development of axonal membrane specializations defines nodes of Ranvier and precedes Schwann cell myelin formation. *J. Cell Biol.* **83**(2, Pt. 2):83a. (Abstr.).
44. WOOD, J. G., D. H. JEAN, J. N. WHITAKER, B. J. MCLAUGHLIN, and R. W. ALBERS. 1977. Immunocytochemical localization of the sodium, potassium activated ATPase in knifefish brain. *J. Neurocytol.* **6**:571-581.